RSC Advances

ROYAL SOCIETY OF CHEMISTRY

www.rsc.org/advances

Journal Name

ARTICLE

Improving Lithium–Sulfur Battery Performance via a Carbon–Coating Layer Derived from the Hydrothermal Carbonization of Glucose

Received 00th January 20xx,
Accepted 00th January 20xx

DOI: 10.1039/x0xx00000x

www.rsc.org/

Songtao Zhang,† Nianwu Li,† Hongling Lu, Jiafei Zheng, Rui Zang and Jieming Cao*

Sulfur possesses high specific capacity as a rechargeable lithium battery cathode. However, the commercial applications of sulfur cathode are limited by the poor electronic/ionic conductivity of elemental sulfur and polysulfides, volume expansion of sulfur during discharge process, and the high solubility of long–chain lithium polysulfides (Li_2S_n, $4 \le n \le 8$). Herein, we design a core–shell structure composed of active carbon (AC) and an amorphous carbon–coating layer to encapsulate the sulfur in the carbon matrix. The carbon–coating layer obtained from the hydrothermal carbonization of glucose can effectively entrap the polysulfides. Furthermore, the composite matrix provides a conducting framework serving as an electrochemical reaction chamber for the sulfur cathode. After wrapped AC–S with an amorphous carbon layer, the obtained composite cathode can effectively confine the polysulfides and buffer the volume change. Consequently, the resulting composite cathode possesses a high specific capacity, good rate capability, and stable cycling performance. At 0.2 A g^{-1} current density, the as–prepared carbon–coated AC–S composite cathode shows a high specific discharge capacity of 1103 mAh g^{-1}. At a current density of 0.8 A g^{-1} and 1.6 A g^{-1}, the composite cathode exhibites 75% capacity retention over 150 cycles. The coulombic efficiency of the cell remains at approximately 95%

Introduction

Rechargeable lithium–sulfur (Li-S) batteries are considered to be promising candidates for advanced energy storage devices because of their high theoretical specific capacity (1,675 mAh g^{-1}) and energy density (2,600 Wh kg^{-1}).[1–7] Furthermore, elemental sulfur also possesses other advantages such as natural abundance, low cost, and environmental benignity.[1] Nevertheless, commercial applications of Li-S batteries have been hindered by several challenges, such as the low electronic/ionic conductivity of elemental sulfur and polysulfides, volume expansion of sulfur during discharge process, and the high solubility of long–chain lithium polysulfides (Li_2S_n, $4 \le n \le 8$) in conventional organic electrolytes.[1,3] The dissolved polysulfides shuttle between the sulfur cathode and lithium anode, causing precipitation of insoluble and insulating Li_2S_2/Li_2S on the surface of the electrodes. This undesirable phenomenon could result in low coulombic efficiency and loss of active materials.[8,9] Various strategies have been explored to address these issues, including optimization of organic electrolytes,[10] fabrication of conductive polymer–sulfur composites,[11–13] and carbon–sulfur composites.[14–18] Porous carbon materials with a high specific surface area, large pore volume, and nanoporous structure were proven to be an effective conductive framework for sulfur cathodes.[19–22] However, polysulfides can still readily diffuse into electrolyte causing the "shuttle" phenomenon.[9, 23] To solve this problem, conductive polymer,[23–25] thin oxide,[26, 27] and reduced graphene oxide [9,28,29] were coated on porous carbon to further trap polysulfides, thereby improving the cycling performance.

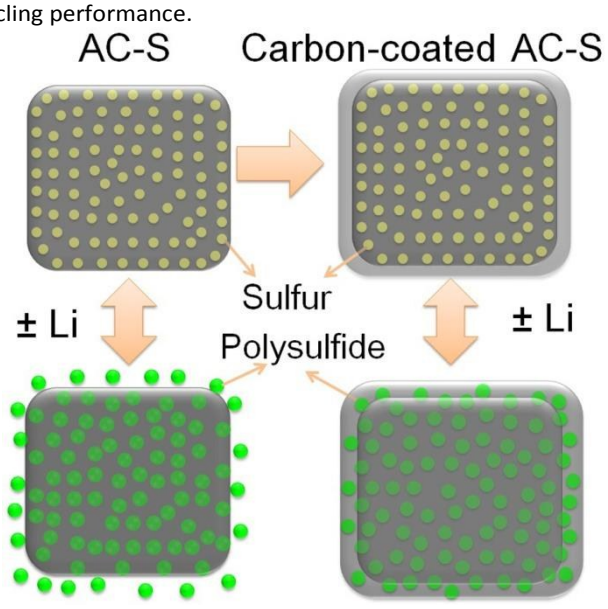

Fig. 1 Schematic of the carbon–coated AC–S composite structure. After wrapped AC–S with an amorphous carbon

Nanomaterials Research Institute, College of Materials Science and Technology, Nanjing University of Aeronautics and Astronautics, Nanjing 210016, China. Fax: +86-25-84895289; Tel: +86-25-84895289; E-mail: jmcao@nuaa.edu.cn
† These authors contributed equally to this work.

layer, the obtained composite cathode can effectively confine the polysulfides and buffer the volume change.

The hydrothermal carbonization of carbohydrates is an easy, low–cost and environment–friendly method to produce amorphous carbon–coating layers,[30–34] which can effectively mitigate the mechanical stress caused by volume change (cushion effect).[30,31] Thus, it has been employed to strengthen the structural integrity of the anode material of lithium–ion batteries.[30–32] Herein, we designed a core-shell structure carbon–coating active carbon–sulfur (AC–S) composite. The amorphous carbon layer derived from the hydrothermal carbonization of glucose was applied to the AC–S composite cathode to improve the electrochemical performance. After wrapped AC–S with an amorphous carbon layer, the obtained composite cathode can effectively confine the polysulfides and buffer the volume change (Fig. 1). The resulting composite cathode exhibited a high discharge capacity of 835 mAh g^{-1} and 75% capacity retention over 150 cycles at 1.6 A g^{-1}.

Experimental

Sample preparation

100 mg of commercial AC was thoroughly mixed and ground with 200 mg of the sublimed sulfur. Afterwards, the mixture was heated to 160 °C and held at this temperature for 24 h to obtain AC–S. The as prepared AC–S composite (100 mg) was dispersed in 1 mL ethanol and 39 mL distilled water, then 280 mg of glucose was dissolved to the suspension with sonication and magnetic stirring. Subsequently, the mixture was aged at 180 °C for 6 h in a Teflon–lined autoclave (hydrothermal treatment process). The obtained product was then washed several times and dried at 70 °C for 24 h under vacuum. The product was nominated as carbon–coated AC–S composite.

Material characterization

X–ray powder diffraction (XRD) patterns were obtained on a Bruker D8 powder X–ray diffractometer (Germany). The microstructure of the samples was examined with a Hitachi S–4800 field–emission scanning electron microscope (FE–SEM) and a JEOL JEM–2100 transmission electron microscope (TEM). The N_2 adsorption–desorption analysis was performed using a Micromeritics ASAP 2010 instrument. Thermal analysis was measured on NETZSCH STA 409C thermal analyzer (Germany), in which the sample was heated in alumina crucible under N_2 flow to 550 °C at a heating rate of 10 °C min^{-1}.

Electrochemical test

The cathode slurry was prepared by mixing 70 wt% of carbon–coated AC–S nanocomposite, 20 wt% of Super P (TIMCAL, Graphite & Carbon Inc.), and 10 wt% of polyvinylidene difluoride (PVDF, Alfa Aesar) dissolved in N–methyl–2–pyrrolidone (NMP, Aldrich). Each current collector contained between 0.9 mg cm–2 to 1.0 mg cm–2 active material. Positive electrodes were produced by coating the slurry on aluminum foil and drying at 60 °C for 12 h. The cell tests was evaluated using 2032 coin–type cells cycled at room temperature between 1.0 V and 3.0 V, which were fabricated in an argon–filled glove box using lithium metal as the counter electrode and a microporous polyethylene separator. The electrolyte was 1 M bis–(trifluoromethane) sulfonamide lithium (LiTFSI) in a mixed solvent of dimethoxyethane (DME) and dioxolane (DOL) with a volume ratio of 1:1. The performance of the cells was tested with LAND CT–2100A instrument (Wuhan, China). The specific capacity was calculated on the mass of elemental sulfur. Electrochemical impedance spectroscopy (EIS) data were obtained with a CHI 760D electrochemical workstation (Shanghai Chenhua, China) by applying a 5 mV amplitude signal from 100 kHz to 10 mHz after charging to 3.0 V.

Results and discussion

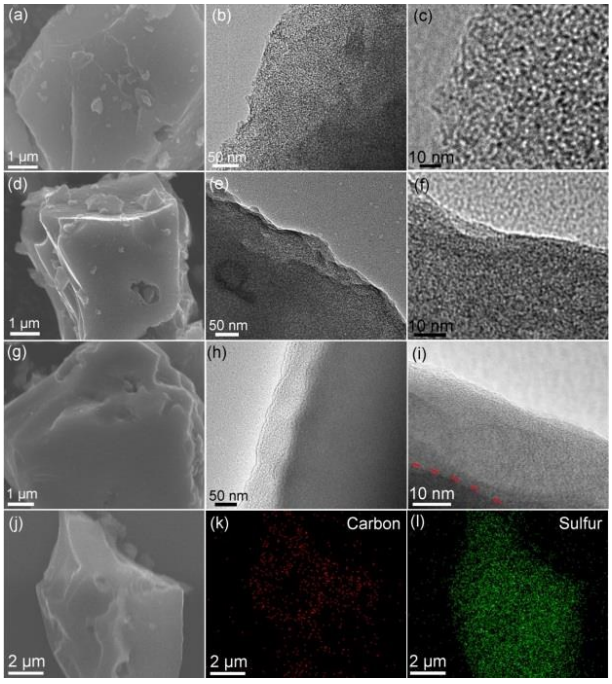

Fig. 2 (a) SEM and (b, c) TEM images of AC; (d) SEM and (e, f) TEM images of AC–S; (g) SEM and (h, i) TEM images of the carbon–coated AC–S composite; and (j) low-magnification SEM image and the corresponding (k) carbon and (l) sulfur mapping of the carbon–coated AC–S composite.

SEM and TEM images of the AC, AC–S, and carbon–coated AC–S composite were obtained to investigate the morphology characteristics. Bulk AC exhibits an irregular structure with the size of several micrometers (Fig. 2a). The TEM images (Fig. 2b and 2c) show that the AC material possesses abundant nanopores homogeneously distributed throughout the particle. In comparison with AC, no apparent difference in the morphology and size of the AC–S composite was found (Fig. 2d). Moreover, no aggregation of bulk sulfur is found on the surface of AC–S composite, which indicates the incorporation of sulfur into the active carbon matrix by a capillary force during the heating process. The TEM image of the AC–S composite (Fig. 2e and 2f) illustrates that the amorphous sulfur phase components are entrapped within the pore channels of the AC matrix. The carbon layer derived from glucose was

coated on the AC–S composite after hydrothermal treatment (Fig. 2g). The TEM image (Fig. 2h) indicates that the AC–S composite is covered with a uniform and continuous amorphous carbon layer. It is worth noting that the amorphous carbon layer contain abundant nanopores (Fig. 2i), which is advantageous for trapping polysulfides.[34] Elemental mapping reveals that elemental sulfur is uniformly distributed in the carbon–coated AC–S composite (Fig. 2k, l).

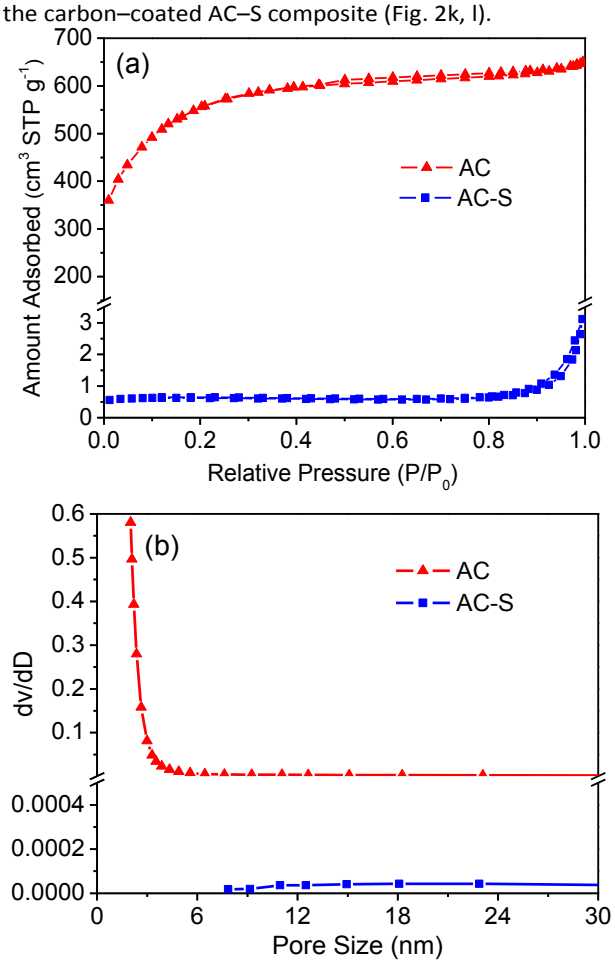

N2 adsorption–desorption analysis was performed to investigate the porous structure of the AC and AC–S composites. The isotherm of AC exhibits a high nitrogen uptake at P/P0 = 0.3 and a small hysteresis at P/P0 = 0.4–0.8 (Fig. 3a), indicating a combined microporous and mesoporous structure of AC.19 The AC matrix shows a high specific surface area of 1880 m2 g–1 and pore volume of 1.01 cm3 g–1 as determined by the Brunauer–Emmett–Teller (BET) method. In theory, 1.0 g AC can accommodate 2.091 g of S (2.07 g cm–3 × 1.01 cm3 g–1, which is the density of S multiplied by the pore volume of the activated carbon), corresponding to a theoretical sulfur loading of 67.6 wt%.35 After encapsulating sulfur in the nanopores, a very low nitrogen uptake at low P/P0 is observed in the nitrogen adsorption–desorption isotherms of AC–S composite. The AC–S composite shows a low BET surface area of 1 m2 g–1 and pore volume of 0.01 cm3 g–1 after sulfur infusion. Such a remarkable decrease in the surface area and pore volume indicates that the sulfur has been embedded into the pores of the AC matrix. The pore size distribution curves obtained using the Barrett–Joyner–Halend- (BJH) method are shown in Fig. 3b. The main peak of the size distribution significantly decreases with the incorporation of sulfur into the AC framework. The XRD patterns of AC, AC–S, and carbon–coated AC–S composites are shown in Fig. 3c. Sharp diffraction peaks of sublimed sulfur indicated that the elemental sulfur exists in a crystalline state. The AC–S composite exhibits significantly lower peak intensities than the pure sulfur, suggesting a poor crystal structure. For the carbon–coated AC–S composite, the sharp diffraction peaks of sulfur nearly disappear, further demonstrating that sulfur exists in a highly dispersed state.9,35 The thermal analysis result (Fig. 3d) shows that the sulfur contents are 65.3% and 57.9% for the AC–S and carbon–coated AC–S composites, respectively.

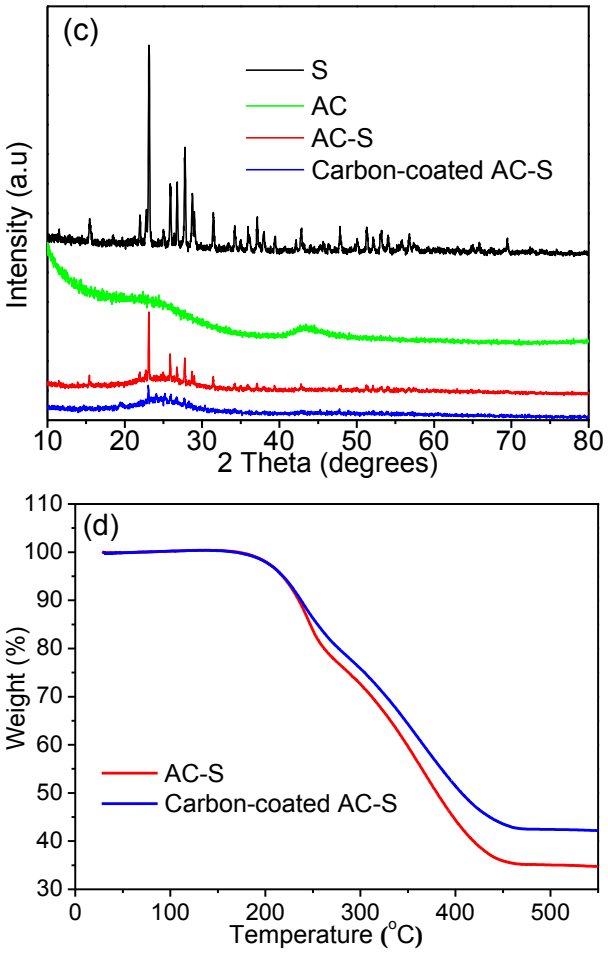

Fig. 3 Nitrogen adsorption–desorption isotherms (a) and B- pore size distribution curves (b) of the AC and AC–S composites; (c) XRD patterns of elemental sulfur, AC, AC–S, and carbon–coated AC–S composites; and (d) Thermal analys- s curves of AC–S and carbon–coated AC–S composites.

The AC–S and carbon–coated AC–S composites we- assembled into Li-S batteries to test their electrochemical

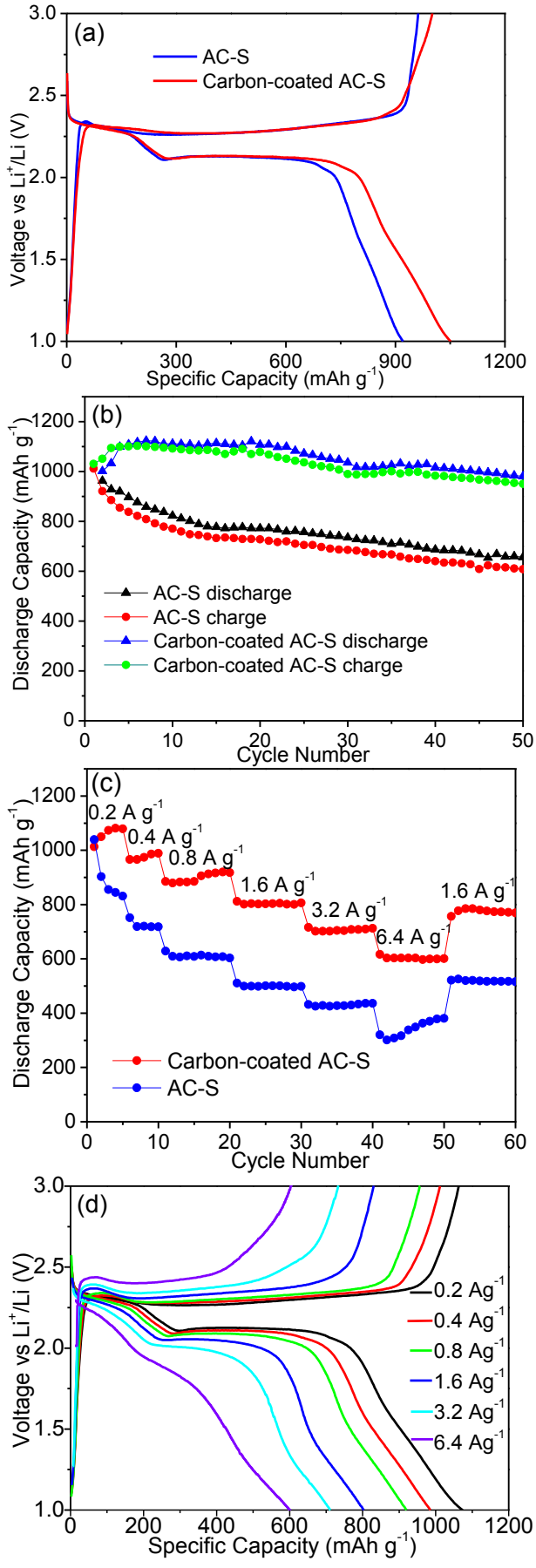

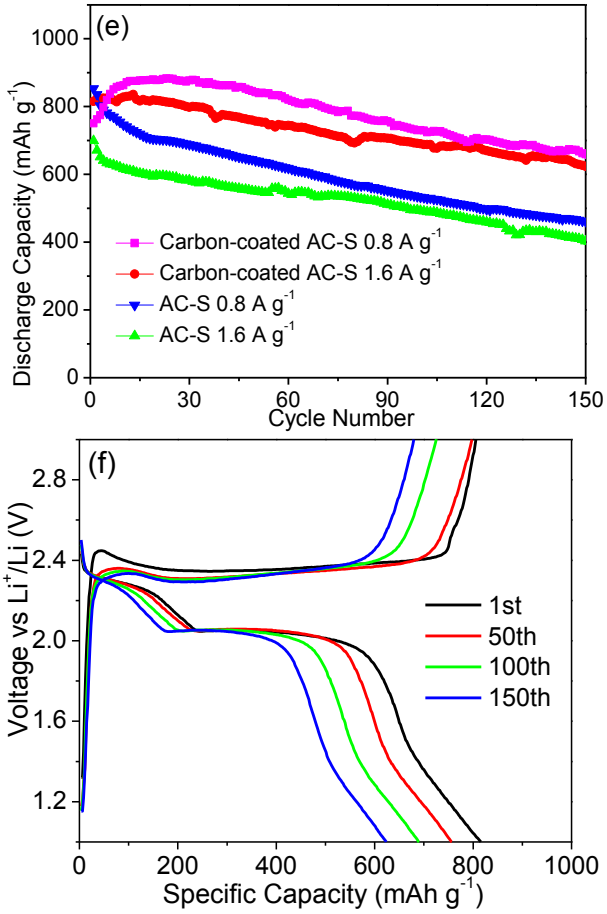

Fig. 4 (a) Discharge/charge voltage profiles and (b) cycle life of the AC–S and carbon–coated AC–S composites at a current density of 0.2 A g^{-1}; (c) Rate capability of AC–S and the carbon–coated AC–S composites; (d) Typical voltage profiles of the carbon–coated AC–S composite; (e) Cycle performance of the carbon–coated AC–S composite at the rate of 0.8 A g^{-1} and 1.6 A g^{-1}; (f) Galvanostatic discharge and charge curves of the different cycles for the carbon–coated AC–S composite at a rate of 1.6 A g^{-1}.

behavior. The typical galvanostatic charge/discharge profiles within a cut–off voltage window of 1.0–3.0 V are shown in Fig. 4a. All the discharge curves display the two–plateau behavior of the sulfur cathode, corresponding to the formation of long–chain polysulfides (Li_2S_n, $4 \le n \le 8$) at ~2.3 V as well as solid-state Li_2S_2/Li_2S at ~2.1 V.[36] The AC–S composite exhibits an initial discharge capacity of 1012 mAh g^{-1} at a current density of 0.2 A g^{-1}. The capacity decreases to 607 mAh g^{-1} after the 50th cycles. The as–prepared carbon–coated AC–S composite possesses an initial specific discharge capacity of 1030 mAh g^{-1}, which increases to 1103 mAh g^{-1} at the 6th cycle, and maintains at 950 mAh g^{-1} after 50 cycles. Although low initial discharge capacities were observed, the carbon–coated AC–S composite showed a gradual increase in discharge capacity during the initial several cycles (Fig. 4b). This behavior indicates that the carbon–coated AC–S composite electrode requires an activation step. A certain amount of time is required for the electrolyte to infiltrate the amorphous

carbon–coating layer.[23,24] This activation phenomenon also occur in other porous carbon–sulfur composite materials.[19] The amorphous carbon layer can effectively inhibit the diffusion of polysulfides during the charge/discharge process, improving the cycle performance of the AC–S electrode. The rate capability study of the AC–S and carbon–coated AC–S composites was conducted at various rates. Compared with AC–S composite, the carbon–coated AC–S compoiste shows a better rate capability behavior. The AC–S composite exhibits a capacity of 379 mAh g^{-1} at a current rate of 6.4 A g^{-1}, while the carbon–coated AC–S composite acquires a capacity of 603 mAh g^{-1} at the same rate (Fig. 4c). When the current rate is increased from 0.2 A g^{-1} to 6.4 A g^{-1}, the carbon–coated AC–S composite maintains the typical two–plateau behavior of the sulfur cathode (Fig. 4d). Furthermore, the discharge capacity can be mostly recovered when the current density is decreased again from 6.4 A g^{-1} to 1.6 A g^{-1}, showing the significant tolerance of the carbon–coated AC–S composite at different current densities. In order to evaluate the cyclability, the samples were tested at 0.8 A g^{-1} and 1.6 A g^{-1} for long life cycle performance (Fig. 4e). The activation phenomena occurs at both rates for the carbon–coated AC–S composite. After amorphous carbon–coating, the resulting composite electrode delivers a maximum reversible discharge capacity of 880 mA h g^{-1} in the 19th cycle at 0.8 A g^{-1} and 835 mA h g^{-1} in the 13th cycle at 1.6 A g^{-1}. The retention rate of the discharge capacity increased from 54% and 57% for the AC–S composite cathode to both 75% for the carbon–coated AC–S composite cathode at 0.8 A g^{-1} and 1.6 A g^{-1}, respectively. At the current rate of 1.6 A g^{-1}, no obvious change in the charge/discharge profiles was observed even after 150 cycles (Fig. 4f). The coulombic efficiency of carbon–coated AC–S composite cathode was maintained at approximately 95%.

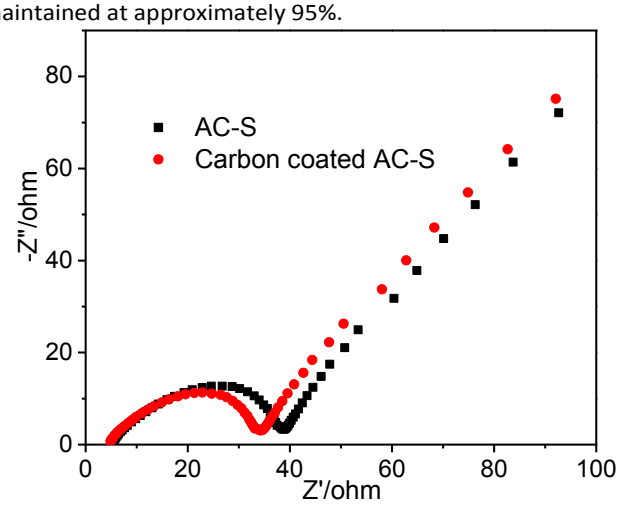

Fig. 5 EIS spectra of AC–S and carbon–coated AC–S composites.

To further investigate the improved electrochemical performance of carbon–coated AC–S composite, EIS spectra of both samples were carried out (Fig. 5). The impedance plots were composed of a depressed semicircle in the high–frequency region and a straight line in the low–frequency region. The semicircle at the high–frequency is related to the charge–transfer process. The straight line at the low–frequency is ascribed to semi-infinite Warburg diffusion process.[37–39] After the amorphous carbon–coating, the charge transfer resistance decrease from 33.3 Ω to 29.5 Ω, probably due to the excellent conductivity of the carbon–coating layer.

The excellent electrochemical behavior of the as-prepared carbon–coated AC–S composite can be attributed to the multiple synergistic factors. First, AC is recognized as a promising matrix for sulfur cathode.[19] Second, the amorphous carbon–coating layer which serves as a microcapsule can further entrap polysulfides during the charge/discharge process as shown in Fig. 1, enabling more stable cycling performance. Third, the amorphous carbon–coating layer provides a buffer region to accommodate volume changes during the charge/discharge process.[32] Therefore, the core–shell structure constituted by AC and carbon–coating layer can serve as a good electrochemical reaction chamber. When assembled into Li-S batteries, the carbon–coated AC–S composite acquires excellent rate capability and long life cycle performance.

Conclusions

In summary, a core–shell carbon–coated AC–S composite was designed for Li-S batteries. The carbon–coating layer obtained from the hydrothermal carbonization of glucose can effectively entrap the polysulfides. Furthermore, the composite matrix provides a conducting framework which can serve as an electrochemical reaction chamber for the sulfur cathode. Consequently, the resulting composite cathode possesses a high specific capacity, good rate capability, and stable cycling performance. Our results demonstrate that the carbon–coated AC–S composite can serve as a promising candidate for Li-S batteries.

Acknowledgements

This work is funded by the Priority Academic Program Development of Jiangsu Higher Education Institutions.

Notes and references

1 A. Manthiram, Y. Fu, S. H. Chung, C. Zu and Y. S. Su, *Chem. Rev.*, 2014, **114,** 11751.
2 V. Etacheri, R. Marom, R. Elazari, G. Salitra and D. Aurbach, *Energy Environ. Sci.*, 2011, **4,** 3243.
3 Y. X. Yin, S. Xin, Y. G. Guo and L. J. Wan, *Angew. Chem. Int. Ed.*, 2013, **52,** 13186.
4 P. G. Bruce, S. A. Freunberger, L. J. Hardwick and J. M. Tarascon, *Nat. Mater.*, 2012, **11,** 19.
5 S. Evers and L. F. Nazar, *Acc. Chem. Res.*, 2012, **46,** 1135.
6 C. Wu, L. Yuan, Z. Li, Z. Yi, Y. Li, R. Zeng, W. Zhang and Y. Huang, *RSC Adv.*, 2015, **5,** 14196.
7 Z. Li, Y. Huang, L. Yuan, Z. Hao and Y. Huang, *Carbon,* 2015, **92,** 41.
8 X. Zhao, M. Liu, Y. Chen, B. Hou, N. Zhang, B. Chen, N. Yang, Y. Chen, J. Li and L. An, *J. Mater. Chem. A*, 2015, **3**, 7870.
9 N. Li, M. Zheng, H. Lu, Z. Hu, C. Shen, X. Chang, G. Ji, J. Cao and Y. Shi, *Chem. Commun.,* 2012, **48,** 4106.

10 D. Aurbach, E. Pollak, R. Elazari, G. Salitra, C. S. Kelley and J. Affinito, *J. Electrochem. Soc.,* 2009, **156,** A694.
11 Y. Z. Fu and A. Manthiram, *J. Phys. Chem. C,* 2012, **116,** 8910.
12 F. Wu, J. Z. Chen, R. J. Chen, S. X. Wu, L. Li, S. Chen and T. Zhao, *J. Phys. Chem. C,* 2011, **115,** 6057.
13 L. F. Xiao, Y. L. Cao, J. Xiao, B. Schwenzer, M. H. Engelhard, L. V. Saraf, Z. M. Nie, G. J. Exarhos and J. Liu, *Adv. Mater.,* 2012, **24,** 1176.
14 N. Jayaprakash, J. Shen, S. S. Moganty, A. Corona and L. A. Archer, *Angew. Chem. Int. Edit.,* 2011, **50,** 5904.
15 C. F. Zhang, H. B. Wu, C. Z. Yuan and Z. P. Guo, X. W. Lou, *Angew. Chem. Int. Edit.,* 2012, **51,** 9592.
16 K. Yang, Q. Gao, Y. Tan, W. Tian, L. Zhu and C. Yang, *Microporous Mesoporous Mater.,* 2015, **204,** 235.
17 G. C. Li, J. J. Hu, G. R. Li, S. H. Ye and X. P. Gao, *J. Power Sources*, 2013, **240,** 598.
18 M. Oschatz, J. T. Lee, H. Kim, W. Nickel, L. Borchardt, W. I. Cho, C. Ziegler, S. Kaskel and G. Yushin, *J. Mater. Chem. A,* 2014, **2,** 17649.
19 S. Zhang, M. Zheng, Z. Lin, N. Li, Y. Liu, B. Zhao, H. Pang, J. Cao, P. He and Y. Shi, *J. Mater. Chem. A,* 2014, **2,** 15889.
20 J. Kim, D. Lee, H. Jung, Y. Sun, J. Hassoun and B. Scrosati, *Adv. Funct. Mater.,* 2013, **23,** 1076.
21 G. He, X. L. Ji and L. Nazar, *Energy Environ. Sci.,* 2011, **4,** 2878.
22 H. Ye, Y. X. Yin, S. Xin and Y. G. Guo, *J. Mater. Chem. A,* 2013, **1,** 6602.
23 Y. Yang, G. H. Yu, J. J. Cha, H. Wu, M. Vosgueritchian, Y. Yao, Z. A. Bao and Y. Cui, *ACS Nano,* 2011, **5,** 9187.
24 G. C. Li, G. R. Li, S. H. Ye and X. P. Gao, *Adv. Energy Mater.,* 2012, **2,** 1238.
25 W. Qin, B. Fang, S. Lu, Z. Wang, Y. Chen, X. Wu and L. Han, *RSC Adv.,* 2015, **5,** 13153.
26 K. T. Lee, R. Black, T. Yim, X. L. Ji and L. F. Nazar, *Adv. Energy Mater.,* 2012, **2,** 1490.
27 M. Yu, W. Yuan, C. Li, J. D. Hong and G. Shi, *J. Mater. Chem. A,* 2014, **2,** 7360.
28 H. Zhao, Z. Peng, W. Wang, X. Chen, J. Fang and J. Xu, *J. Power Sources*, 2014, **245,** 529.
29 S. Liu, K. Xie, Y. Li, Z. Chen, X. Hong, L. Zhou, J. Yuan and C. Zheng, *RSC Adv.,* 2015, **5,** 5516.
30 X. W. Lou, C. M. Li and L. A. Archer, *Adv. Mater.,* 2009, **21,** 2536.
31 W. M. Zhang, X. L. Wu, J. S. Hu, Y. G. Guo and L. J. Wan, *Adv. Funct. Mater.,* 2008, **18,** 3941.
32 X. W. Lou, D. Deng, J. Y. Lee and L. A. Archer, *Chem. Mater.,* 2008, **20,** 6562.
33 F. Qin, K. Zhang, L. Zhang, J. Li, H. Lu, Y. Lai, Z. Zhang, Y. Zhou, Y. Li and J. Fang, *Dalton. Trans*., 2015, **44,** 2150.
34 H. Wang, Z. Chen, H. K. Liu and Z. Guo, *RSC Adv.,* 2014, **4,** 65074.
35 X. Ji, K. T. Lee and L. F. Nazar, *Nat. Mater.,* 2009, **8,** 500.
36 J. J. Cheng, Y. Pan, J. A. Pan, H. J. Song and Z. S. Ma, *RSC Adv.,* 2015, **5,** 68.
37 S. R. Narayanan, D. H. Shen, S. Surampudi, A. I. Attia and G. Halpert, *J. Electrochem. Soc.,* 1993, **140,** 1854.
38 Z. Deng, Z. Zhang, Y. Lai, J. Liu, J. Li and Y. Liu, *J. Electrochem. Soc.,* 2013, **160,** A553.
39 Y. Huang, M. Zheng, Z. Lin, B. Zhao, S. Zhang, J. Yang, C. Zhu, H Zhang, D. Sun and Y. Shi, *J. Mater. Chem. A*, 2015, **3**, 10910.

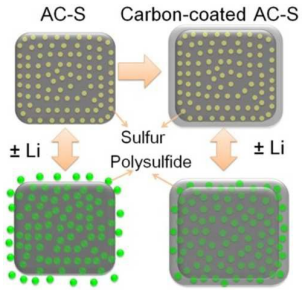

After wrapped AC–S with a carbon–coating layer, the obtained composite can effectively confine the polysulfides.